0038-075X/92/1532-0129$03.00/0
SOIL SCIENCE

February 1992
Vol. 153, No. 2
Printed in U.S.A.

MOISTURE EFFECTS ON VISIBLE SPECTRAL CHARACTERISTICS OF LATERITIC SOILS

ALI BEDIDI,[1] BERNARD CERVELLE,[1] JOSÉ MADEIRA,[2] AND MARCEL POUGET[2]

Samples from ferralitic soils of similar texture were immersed in water, placed in a pressure chamber and subjected to different soil suction pressures (pF: 2.0, 2.5, 2.8, 3.0, and 4.2). The Cie color values (intensity, hue and saturation) were taken as the spectral signatures of these soils and calculated from the diffuse reflectance spectra. The dominant wavelength λ_d (hue) increases with moisture content; as the soil becomes more "colored" by iron oxi-hydroxides, this increase becomes more pronounced. The purity Pe (saturation) decreases systematically with increasing moisture content. When the moisture content increases, i.e., from oven-dried to air-dried and then to moist samples, there is a change of the refractive index, N, of the immersion medium from $N = 1$ (air) to $N = 1.33$ (water). This change causes an increase in the volumetric reflectance, especially in the weak absorption regions, and a decrease in the specular reflectance. Contrary to the generally accepted assumption, diffuse reflectance spectra of soils at different moisture contents undergo nonlinear changes leading to displacements in the spectral extrema of the absorption bands. Therefore, spectral signatures of moist soils cannot be derived simply from those of their dry equivalents.

The color of the surface of a soil depends, among other factors, on its mineralogical composition, its surface morphology, and its moisture level, all of which strongly modify the intrinsic spectral properties of mineral compounds. Rainfall has many effects on soil color since it modifies surface roughness (Bertuzzi et al. 1990; Boifin 1984; Mitchell and Jones 1978) inducing directional variations of reflectance spectra (Cierniewski 1983, 1987). Heavy rainfalls cause soil erosion and separation; on one hand, fine materials are deposited at the bottom of slopes, and, on the other, coarse materials emerge at the surface and influence the reflection of the solar radiation. Finally, water causes soil swelling and changes in structure (Braudeau 1988; McGarry and Daniels 1987; Giraldez et al. 1983) thus inducing complex reflectance changes.

Study and modeling of the effect of water action on soil spectral characteristics help in the interpretation of remotely-sensed data. Water is largely responsible for the variability of agronomic parameter measurements; furthermore, moisture and shadow effects may be confused in remote sensing measurements (Epiphanio and Vitorello 1984). Therefore, geographers have problems when they make stereographic reconstructions of the relief.

Moisture content and hydric potential are data of interest for environmental and agronomic purposes. In this work, we have studied the diffuse reflectance variations, in the visible range from 400 nm to 770 nm, and color variations (Cierniewski 1985; Prost et al. 1983; Shields et al. 1968) of lateritic soil samples with different moisture levels. It should be noted that this type of soil represents more than 20% of pedologic cover at land surface (Bocquier et al. 1984). The reflectance variations due to moisture were related to the hydric potential of soils, and a close relation was found between these reflectance variations and the distribution of water into the different pores of the soil samples.

MATERIALS AND METHODS

Soil Samples

Origin

The soil samples used in this study come from the surface horizons (Ap) of ferralitic and hydromorphous soil toposequence which derive from pre-Cambrian siltites located in Brasilia (Brazil). According to the Brazilian criteria (Camargo et al. 1987) the sampled soils are classified as (1) latosol vermelho escuro (dark red latosol),

[1] Laboratoire de Minéralogie-Cristallographie, Universités P. et M. CURIE et PARIS 7, Tour 16, 4 Place Jussieu, 75252 Paris Cedex 05, France.
[2] Unité de Télédétection, Centre ORSTOM-Bondy, 70 Route d'Aulnay, 93143 Bondy, France.
Received Dec. 14, 1990; accepted March 14, 1991.

(2) latosol vermelho amarelo (red yellow latosol), (3) laterita hidromorfica (hydromorphic laterite), and (4) gley pouco humico (low humic gley).

Preparation

The aggregates were hand-broken with finger pressure, and the samples were sieved (2 mm) without grinding. Each sample was divided into three portions: the first one was used for the determination of the organic matter (titration with 0.1 N $FeSO_4$ after oxidation by 0.4 N $K_2Cr_2O_7$ (EMBRAPA 1979), the total iron content (triacid extraction) (Harrisson 1933), free iron oxides content (Citrate-bicarbonate-dithionite extraction as described by Mehra and Jackson 1960), and amorphous iron oxides (extraction by TAMM solution:ammonium oxalate-oxalic acid) (Schwertmann 1964). A second portion was used for the grain size analysis by the pipette method, after dispersion in a solution of NaOH, and a third portion was used for reflectance measurements at different moisture contents.

Preparation of moist samples

After water saturation, the samples were put in a tension room and processed to the moisture contents corresponding to several suction pressures (pF: 2.0, 2.5, 2.8, 3.0, and 4.2). Two other moisture levels were considered: oven-dry at 105°C for 24 hours and air-dry. Each moist sample was divided into three parts which were put together in the tension room; the first one was used for the moisture rate measurement and the two others for reflectance measurements. To avoid moisture losses before reflectance measurement, samples were placed in a freezer at 4°C. They were brought to normal room temperature 15 to 20 min. before each spectrum recording. To evaluate the possible moisture losses, the spectrum of each moist sample was measured twice, the second measurement being carried out 30 min. after the first one. Table 1 shows the moisture contents corresponding to the tensions used for the four samples. The sample pairs (1–4) and (2–3) have very close moisture rates at each tension, which is due to their textural resemblance. Use of the same tensions has the advantage that water fills the same pore-space for all the samples. As the soils studied are poor in soluble salts, the scattering media can be considered to be the same for all the samples at a given tension.

Diffuse Reflectance Spectra Measurements

The reflectance spectra of the samples were recorded with a CARY 2300 spectrophotometer equipped with an integrating sphere the interior of which is coated with Halon (Halon is a white standard with absolute reflectance up to 99% in the visible range). The spectra were measured from 400 to 770 nm in 5-nm steps, the diffuse reflectance being calculated against a plate of Halon as a reference. Each soil sample was put in an aluminum sample holder with a circular hole of 2 cm in diameter and 2 mm in depth. The surface of the sample was gently leveled and covered with an optically treated silica lamella (0.5 mm thick, 92% transmission) to avoid the particulate sample falling into the integrating sphere. Despite the transparency of the silica lamella in the visible range, it induces changes in the reflectance spectra that must be studied and for which a model has been developed. These changes are due to the dependence of the lamella reflexion coefficient on the incidence angle of the light beam.

Silica Lamella Effects

The use of the silica lamella introduces reflectance changes that are difficult to predict. This

TABLE 1

Suction pressure, moisture content and diameter of the water-filled pores

Pressure		Moisture content (weight%)				Water-filled pores diameter (μm)
pF	Bar	1	2	3	4	
4.2	160	19.4	17.0	16.7	19.0	≤0.009
3.0	1.00	21.8	19.7	18.8	21.1	≤1.5
2.8	0.63	23.3	21.5	20.2	23.0	≤2.4
2.5	0.32	26.9	24.5	23.8	26.3	≤4.7
2.0	0.10	32.0	29.8	28.9	30.9	≤15
Air-dry		2.1	2.0	1.9	2.5	

change in reflectance depends on the lamella used, on the reflectance level of the sample and on the sample reflectance indicatrix which characterizes the variation of reflectance with respect to the incident light and view directions. Despite the transparency of the lamella in the wavelength range of the study, the reflectance changes induced are theoretically wavelength dependent because of their dependence on the reflectance level and the reflectance indicatrix. If i is the angle of incidence relative to the sample surface normal, one can characterize the lamella by a reflexion coefficient, $r(i)$, and a transmission coefficient, $t(i)$, and the sample by a bidirectional reflectance $R(i, i')$ where

$$R(i, i') = R_0 g(i, i') \tag{1}$$

with the i angle of incidence, the i' angle of reflection, and R_0 the directional-hemispheric reflectance and g the reflectance indicatrix which is supposed to be dependent only on the angles of incidence (i) and of reflection (i'). We find:

$$\begin{aligned} I_r = {} & I_0 r(i) + I_0 t(i) R_0 \int_{\Omega'} g(i, i') t(i')\, d\Omega' \\ & + I_0 t(i) R_0^2 \int_{\Omega'} g(i, i') r(i') \\ & \int_{\Omega''} g(i', i'') t(i'')\, d\Omega''\, d\Omega' \\ & + I_0 t(i) R_0^3 \int_{\Omega'} g(i, i') r(i') \\ & \int_{\Omega''} g(i', i'') r(i'') \\ & \int_{\Omega'''} g(i'', i''') t(i''')\, d\Omega'''\, d\Omega''\, d\Omega' + \cdots \end{aligned} \tag{2}$$

where $d\Omega'$ is the solid angle element in the i' direction.

Equation (2) cannot be used because it requires the knowledge a priori of the reflectance indicatrix g. If one assumes that the sample is lambertian, i.e., it reflects light in the same amounts in all directions and independently of the incident beam direction (see Wendlandt and Hecht 1966), then the reflectance indicatrix can be written:

$$g(i, i') = \cos(i)\, \cos(i') \tag{3}$$

$\cos(i)$ and $\cos(i')$ are used here to account for orientation of the observed surface relatively to incident and viewing directions. Using equation (3), equation (2) becomes:

$$I_r = I_0 r(i) + I_0 t(i) \cos(i) \bar{t}\, \frac{R_0}{1 - \bar{r} R_0} \tag{4}$$

with:

$$\bar{r} = \int_{\Omega} [\cos(i)]^2 r(i)\, d\Omega \text{ and} \tag{5}$$

$$\bar{t} = \int_{\Omega} \cos(i) t(i)\, d\Omega$$

The spectrophotometer used in this study has an incident radiation beam normal to the sample surface, so $i = 0$, and the integrating sphere is so built that the specular component ($I_0 r(i)$) is removed from it and not taken into account in the reflectance measurement. Therefore equation (4) becomes:

$$R_L = R_0\, \frac{t(0)\bar{t}}{1 - \bar{r} R_0} \tag{6}$$

where R_L is the ratio I_r/I_0. The validity of this formula has been tested using six compact samples. Results are shown in the results and discussion section.

Color Measurements

To quantify the color of the different moist samples and to study its variation with moisture content we have chosen to use the Cie-colorimetric system. This system has the advantage of offering a measurement of very low variability and a high reproducibility since the measurement is derived from reflectance spectra and is independent of the observer. A short description of this system is given below. For more details see Wyszecki and Stiles (1982) and Cervelle et al. (1977) for application to mineral powders.

Cie-1931 colorimetric system

The first Cie-1931 Standard Observer is characterized by three matching functions $\bar{r}(\lambda)$, $\bar{g}(\lambda)$, and $\bar{b}(\lambda)$ corresponding to the colorimetric aptitudes of the human eye to red, green, and blue stimuli, respectively. Since the function $\bar{r}(\lambda)$ takes negative values for some wavelengths, the design of a colorimetric measurement apparatus is very difficult. Therefore the Cie defined another system of three "primary colors," or stim-

uli, which have no physical reality, but its corresponding matching functions $\bar{x}(\lambda)$, $\bar{y}(\lambda)$, and $\bar{z}(\lambda)$ take only positive values over the visible wavelength range.

Besides the eye response, the photons incident on the eye have a spectral distribution of their energies which has an important role in the determination of colors. The different light sources can be characterized by their spectral power density.

The photons emitted by a given source are either directly collected by the eye, or first reflected by an object having a reflectance spectrum $R(\lambda)$ and then collected by the eye. Other situations can occur where multiple reflections and transmissions of the photons by different objects occur before they are collected by the eye. Consequently, color depends simultaneously on the three contributions: the light source, the object illuminated by this source and observed by the eye, and, lastly, the complex of human eye and brain which is sensitive to the light within the wavelength range 400 nm to 770 nm.

Color has a three-dimensional character and can be quantitatively expressed by two rectangular coordinates located in a plane, called the chromaticity coordinates, and an intensity supported by an axis perpendicular to the plane, and which corresponds to the luminance.

Quantitative expression of chromaticity coordinates and luminance

The color of an object with a reflectance spectrum $R(\lambda)$ within 400–770 nm range, lit by a source of spectral power density $S(\lambda)$, can be characterized by the tristimuli X, Y and Z:

$$X = \int_{380nm}^{770nm} \bar{x}(\lambda)S(\lambda)R(\lambda)\, d\lambda \qquad (7)$$

The chromaticity coordinate: x is defined by:

$$x = \frac{X}{X + Y + Z} \qquad (8)$$

Similar equations will be used to compute Y, Z and y, z.

Since $x + y + z = 1$, only x and y are retained and are called the chromaticity coordinates. The color intensity is characterized by the luminance $Y\%$, defined by:

$$Y\% = 100 \cdot \frac{\int_{380nm}^{770nm} \bar{y}(\lambda)S(\lambda)R(\lambda)\, d\lambda}{\int_{380nm}^{770nm} \bar{y}(\lambda)S(\lambda)\, d\lambda} \qquad (9)$$

It represents the brightness of the color. Integrals were replaced by discrete sums with step intervals of 5 nm in computation.

Because the chromaticity coordinates are not visually meaningful, Helmholtz coordinates have been introduced here: the dominant wavelength (λ_d) which is related to the hue, and the purity (Pe) which is related to saturation. To show the meaning of the dominant wavelength and the purity and their relationship to the chromaticity coordinates, it is helpful to use the chromaticity diagram.

Chromaticity diagram, dominant wavelength, and purity (Fig. 1)

In a rectangular representation each couple of chromaticity coordinates (x, y) is represented by a point. The points corresponding to the colors of all the visible monochromatic radiations are located on a line which is called the spectrum locus. This curvilinear line is scaled in wavelength and is closed by the purple line which joins the red-end to the blue-end of the spectrum locus. The spectrum locus defines a triangular-shaped closed surface called the chromaticity diagram. All real colors fall within this triangle.

The C-illuminant (Cie Standard corresponding to the average day light) radiates a white light whose chromaticity coordinates are $x = 0.3101$ and $y = 0.3162$, corresponding to a point located almost at the center of the diagram, where the three primary stimuli are in equivalent proportions.

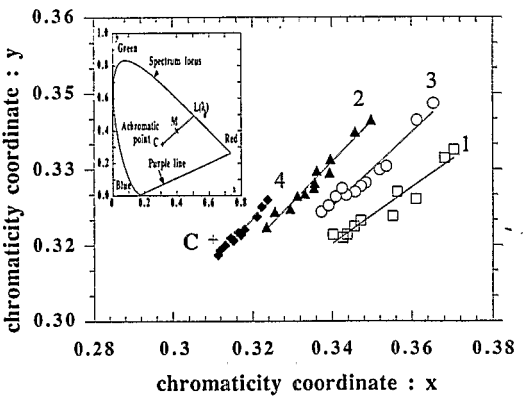

FIG. 1. Chromaticity coordinates, x and y, of the four soil samples. 1 (□), 2 (△), 3 (○) and 4 (♦), for different moisture states. Ov.-dry: oven-dried sample at 105°C for 24 h. In the upper left corner, the chromaticity diagram.

On the chromaticity diagram, the extension of a straight line from the point C, representing the C-illuminant, through the point M, representing the object under consideration, intersects the spectral locus at a point L which corresponds to the dominant wavelength $\lambda_d(C)$. It is the "hue" of the object illuminated by the C-illuminant. The same object illuminated by the A-illuminant will have another dominant wavelength $\lambda_d(A)$. The ratio of the CM segment length to the CL segment length gives the purity Pe. When the point M is near λ_d (Pe $\rightarrow$ 100%) the color is saturated, i.e., nearly pure, and when it is near the point C (Pe $\rightarrow$ 0%) the color is faded, i.e., strongly mixed with white or grey.

In this new representation of color (λ_d, Pe), the luminance Y% defined by the equation (9) keeps its meaning. The chromaticity diagram and the luminance axis define a pyramid-like volume which corresponds to the volume of colors. The luminance takes then the value 100% within the chromaticity diagram, and the value 0% at the apex of the pyramid. The apex corresponds to the absolute black, i.e., the absence of visible light.

To give an idea about change in color induced by reflectance variation, we have made some simple calculations which show that:

1) if a visible reflectance spectrum $R_0(\lambda)$ is homotheticaly (multiplied by a constant) changed to $R(\lambda)$, $R(\lambda) = \alpha \cdot R_0(\lambda)$, then only the luminance changes from Y% to αY%, λ_d and Pe remain constant;

2) If $R_0(\lambda)$ is linearly changed to $R(\lambda) = \alpha \cdot R_0(\lambda) + \beta$, then λ_d remains constant, Pe changes (formula not shown) and Y% changes to $\alpha Y\% + \beta$.

Since α and β are constants any change in the dominant wavelength is a consequence of non-linear changes in reflectance.

RESULTS AND DISCUSSION

Soil Properties

Table 2 shows that the four samples are clayey (<2 μm). One must note that it is not easy to determine the real grain size distribution of lateritic soils. The silt fraction is not constituted by individual grains, but, in general, the "grains" are aggregates of kaolinite crystallites and oxy-hydroxides which in fact have sizes less then 2 μm. The results of the grain size analysis depend on the grain dispersion method used (Cambier and Prost 1981, Guidez and Langohr 1978).

The organic matter content differs little between samples. Color and iron contents are the most variable characteristics between samples. Most of the iron present is free iron. Crystalline iron oxides, which can be estimated by the difference between free iron and amorphous iron contents, constitute most of the free iron oxides. Hematite and goethite are the constituents of this crystalline form as confirmed by X-ray diffraction. The color is due to the different concentrations in iron oxides and oxy-hydroxides. The redness of soils is attributed to the hematite concentration (Barron and Torrent 1986; Torrent et al. 1983). Macedo and Bryant (1987) have demonstrated, in a pedosequence study, that color in oxisols changed from red to yellow when hematite content decreases. This is the case of the samples studied.

Reflectance Spectra

Although the soils studied are clayey and absorbing, measurements were made to test if the depth of the sample layer (2 mm) is great enough to avoid the possibility that some photons reach the aluminum bottom of the sample-holder and then are reflected back. For this purpose, the soil sample (1) has been put between two silica

TABLE 2

Selected physical and chemical characteristics of the soil samples. CBD: Citrate-bicarbonate-dithionite extraction). TAMM: extraction by TAMM solution (0.175 M Ammonium oxalate-0.1 M oxalic acid)

Sample	Munsell color	Grain-size (%)			Organic carbon (%)	Iron (%)		
		Clay	Silt	Sand		Total	CBD	TAMM
1	2.5YR 4/4	55.1	16.5	26.2	1.70	7.25	6.30	0.28
2	10YR 5/3	47.3	21.6	28.4	2.08	3.75	3.00	0.40
3	7.5YR 4/4	48.7	18.0	31.9	1.90	4.75	3.85	0.32
4	10YR 4/1	62.4	18.1	18.3	2.05	1.77	0.95	0.24

lamellae separated by a space 2 mm wide and its transmission spectrum measured.

For an incident beam of unit intensity let T_1 be the intensity of light transmitted through the first lamella and the sample (that is the intensity of light that would reach the bottom of the sample holder), let t be the transmission of the lamella ($t = 0.92$), and T_2 be the intensity of light that would pass through the sample and the two lamellae. Then

$$T_2 = t \cdot T_1$$

The measurement of T_2 gave the result: 0.00% transmission over all the wavelength range studied. That is $T2 = 0.0000$.

Thus, $T2 < 10^{-4}$ that implies $T1 < 0.000109$ value which is largely below error limits. Consequently, no photons reach the bottom of the sample-holder, and all the incident radiation interacts only with soil samples.

Silica lamella effects

To test the validity of equation (6), and thus the validity of the lambertian reflexion hypothesis, six compact samples (E1 to E6) have been chosen with different levels of reflectance (Table 3). The reflectance spectra of these samples have been recorded both without using the lamella (R_0) and with the lamella covering the samples (R_L). Equation (6) shows that the relation between R_L and R_0 depends only on three constants characteristic of the lamella: $t(0)$, $\bar{t}$, and $\bar{r}$. These constants are independent of wavelength (the transmission of the lamella is constant, 92%, over all the wavelength range of the study). Therefore the plots of R_L/R_0 against R_0 for all the test samples and all wavelengths must lie on the same curve determined by the equation (6). However, as illustrated on Fig. 2, the behavior of R_L/R_0 versus R_0 differs for each of the test samples (E4, E5, and E6). It should be noted that sample E5 has a reflectance spectrum very similar to those of our soil samples. Therefore the equation (6) is an insufficient approximation.

Theoretical calculations were made to correct the soil reflectance from the lamella effects. But, since the formula derived (Eq. 6) is not satisfactory, a pragmatic approach has been adopted: the variation in the colorimetric parameters (λ_d, Pe, and Y%) due to the lamella on the test samples have been compared with the variations of the same parameters due to moisture on our soil samples. The results of this comparison,

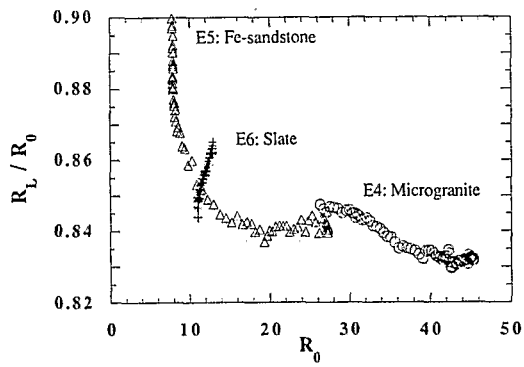

FIG. 2. Variations of R_L/R_0 versus R_0 for the three test samples E4, E5, and E6. R_L: reflectance of the sample covered by the lamella. R_0: reflectance of the sample alone. These samples do not follow the relation given by equation (6) in the text which shows the need of taking into account directional effects.

TABLE 3

Test samples used to evaluate the effect of the silica lamella on reflectance spectra and on color. Only the slate sample has a reflectance which decreases from the blue to the red region.

Sample	Description	R_{min}, %	R_{max}, %	λ_d, nm	λ_d*, nm	Pe, %	Pe*, %	ΔPe/Pe, %	Y, %	Y*, %	ΔY/Y, %
E1	$BaSO_4$ plate	93.5	98.5						97.2	93.0	−4.32
E2	$BaSO_4$ oven-dried powder	94.1	96.5						95.4	86.9	−8.91
E3	$BaSO_4$ wet powder	91.6	95.5						92.9	84.9	−8.61
E4	Microgranite (sawn face)	26.3	45.4	580.0	580.0	13.5	12.8	−5.19	37.9	31.6	−16.62
E5	Fe-sandstone (sawn face)	7.7	27.4	601.0	601.0	22.4	20.3	−9.38	10.7	9.2	−14.02
E6	Slate (freshly cut face)	10.9	12.9	480.0	480.0	3.6	4.0	11.11	12.1	10.4	−13.31

Rmin: reflectance minimum; Rmax: reflectance maximum; λ_d, Pe, Y: dominant wavelength, purity, and luminance calculated from the spectra recorded without the lamella. λ_d*, Pe* and Y* calculated from the spectra of samples covered with the lamella. ΔPe/Pe, ΔY/Y: respectively, changes in purity and luminance relatively to oven-dry sample

summarized as follows, are discussed in results of color measurements.

1) the lamella induces no changes in ("hue") dominant wavelength (Table 3)

2) the relative variation of purity due to the lamella is 10 times less important than that due to moistening;

3) the lamella leads to variations of luminance which are of the same order due to moistening.

Spectra description

Features in visible spectra of minerals are generally attributed to charge transfer and crystal-field absorption bands of Fe^{3+} in octahedral sites (Maquet et al. 1981). The visible diffuse reflectance spectra of the four soil samples are presented in Figs. 3a to 3d. Reflectance between 400 to 770 nm decreases from the dry to the pF 4.2 sample. This decrease is stronger in the red region (around 650 nm) than in the green region (around 540 nm) or blue region (around 420 nm). When pF decreases (i.e., moisture content increases), reflectance changes differ from one wavelength to another and from one soil to another (Figs. 4a and 4b):

a) In the red region, the reflectance of soils 1, 2, and 3 decreases and goes through minima located, respectively, at pF 2.5, 2.8 and 2.8. The reflectance of soil 4 presents a minimum at pF 4.2.

b) In the green and blue regions the reflectance has a minimum at pF 4.2.

Cierniewski (1985) observed a minimum of the reflectance at pF 1–1.5, but the soils he has studied were podsolic and degraded black earths.

This wavelength-dependent behavior of moist soil reflectance gives rise to spectra crossings

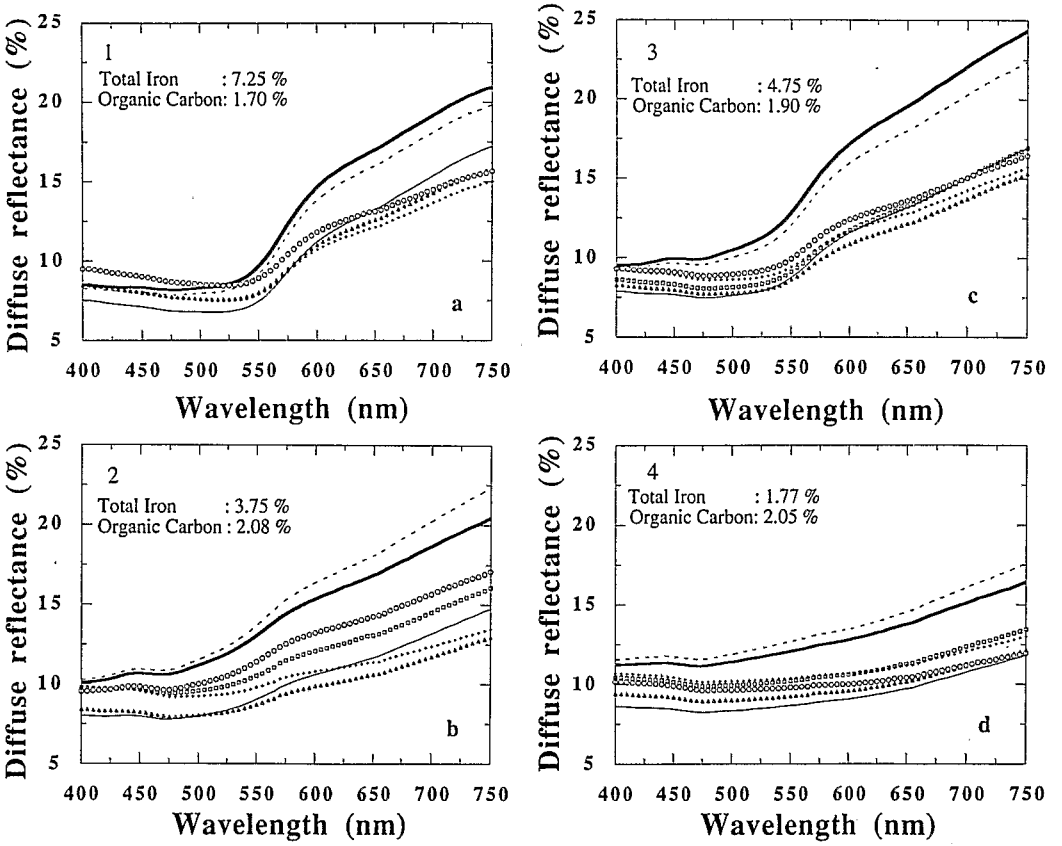

FIG. 3. Variation of the diffuse reflectance spectra, between 400 and 700 nm, for the samples 1(a), 2(b), 3(c), and 4(d), and for the different moisture states: oven-dried (—), air-dried (– – –), pF 4.2 (—), pF 3.0 (□), pF 2.8 (△), pF 2.5 (+), and pF 2.0 (○). The total iron and organic carbon contents are reported on the top left-hand corner.

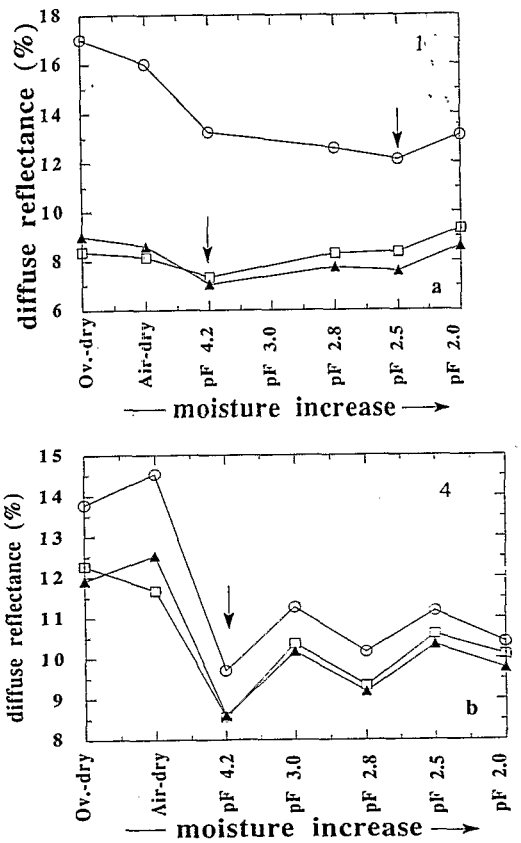

FIG. 4. Variation of the diffuse reflectance of the samples 1(a) and 4(b), for the different moisture states, and at the wavelengths: 650 nm (○), 540 nm (△) and 420 nm (□). Arrows indicate the reflectance minima.

located in the green region as well as to a displacement in reflectance minima located near 540 nm towards longer wavelengths. This displacement leads to the increase in the dominant wavelength as will be shown in the next section. In fact, it is the whole reflectance shoulder located near 540 nm which is shifted towards the longer wavelengths. For example, the minimum of reflectance of the soil (1) is displaced from 475 nm for the oven-dry sample to 520 nm for the sample at pF 2.8 (Fig. 5).

For each sample a second reflectance spectrum was recorded 30 minutes after the first one. Small differences in reflectance and color parameters between the two have been noticed. These differences are due to the drying of the samples and so to changes in moisture content.

Variations of reflectance during sample drying

To give an interpretation of the spectral behavior of the samples when their moisture content changes, we must first try to answer two questions. First, where is the water located in the soil? and second, what "optical" changes are induced by the water? To answer the first question it is useful to present and describe the shrinkage curve.

The shrinkage curve of a soil The shrinkage curve represents the soil volume per unit mass of solids against the gravimetric water content during drying (Braudeau 1988; McGarry and Daniels 1987; Giraldez et al. 1983). A soil presents two systems of porosity: the pores within the grains and aggregates, which constitute the microporosity, and the pores and space between the grains and aggregates, which constitute the macroporosity. When a soil sample dries, it goes through the following stages:

1) water first evacuates the macropores and is gradually replaced by air,

2) the microporosity begin to be evacuated in its turn but without air entering,

3) a point C is reached where the macroporosity is completely water-free,

4) the evacuation of the microporosity continues without air-entry and the sample is rapidly subjected to strong shrinkage,

5) A point B is reached where air begins to fill the microporosity which continues to evacuate its water until the sample is "completely" dry.

Optical interpretation Let us first compare the dry state to the water saturated state. The main optical change is the increase in the im-

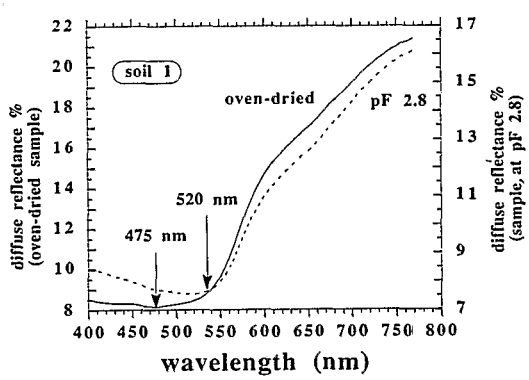

FIG. 5. Displacement of the reflectance shoulder near 540 nm of sample 1 at pF 2.8 (– – –) relatively to oven-dried state (—).

mersion medium index of refraction from $N = 1$ for air to $N = 1.33$ for water. This increase is followed by a change in the scattering properties of the grains and in the balance between absorption and scattering. Bohren (1987) has shown that adding water to sand increases the forward scattering (here the word forward is relative to the direction of the light incident on the grain after multiple scattering and not to the direction of the original incident beam on the sample). As Vincent and Hunt (1968) reported, the total reflectance (Rt) of a particulate medium is the sum of a specular component (Rs) and of a volumetric component (Rv). For an incident beam of unit flux, the specular reflectance is the sum of all the photons reflected at the surface of the grains and the volumetric reflectance is the sum of all the radiation reflected after passing through the grains. The relative amounts of Rs and Rv in the total reflectance is governed, on one hand, by the optical (refractive and absorption indices) and geometrical (size and shape) properties of the grains, and on the other, by the optical properties of the surrounding medium. To give an idea about these phenomena let us consider grains with large sizes (diameter $\gg$ wavelength) and smooth surfaces (wavelength $\gg$ standard deviation of the surface undulations). In this case, the specular reflectance can be described by Fresnel's equation for mirror-like reflectance:

$$R_s = \frac{(n - N)^2 + n^2k^2}{(n + N)^2 + n^2k^2} \qquad (10)$$

where n is the refractive index of the grain, k its absorption index, and N the refractive index of the surrounding medium. Equation (10) indicates that: (i) when N increases (air $\rightarrow$ water) the specular reflectance decreases, and (ii) when absorption is strong (high values of k) the specular reflectance approaches unity. Likewise, the transmittance at the grain surface is given by Fresnel's equation for transmission:

$$T = \frac{4nN}{(n + N)^2 + n^2k^2} \qquad (11)$$

Equation (11) indicates that first the transmittance increases when N increases, leading to an increase of the volumetric reflectance when the surrounding medium changes from air to water. Even if the grain is absorptive the amount of light transmitted through the grain is larger when it is surrounded by water than when it is surrounded by air; this can be explained using Lambert's law: for a radiation of intensity I_0 penetrating the volume of an absorptive medium of thickness d and of absorption coefficient α, the intensity, I, of the transmitted light is given by:

$$I = I_0\exp(-\alpha d) \qquad (12)$$

If the intensity of the radiation penetrating the volume increases, that is I_0 increases to $I_0 + \delta$, then the transmitted light increases by $\delta \exp(-\alpha d)$ according to Lambert's law. Therefore the volumetric reflectance increases.

Second the transmission decreases for strong absorption, and it approaches zero for very high values of k. Thus, water immersion has opposite effects for specular and for volumetric reflectances.

Hunt and Vincent (1968) have studied the behavior of some powdered minerals' reflectance with grain size and have found three types of absorption bands: a first band type where the specular component of the reflectance dominates, a second type where the volumetric component dominates and a third type where the dominance swings from the specular component to the volumetric component. For lateritic soils, the dominance of the specular or the volumetric components is also governed by the intensity of the absorption of hematite and goethite bands present in red, green, and blue regions of the visible spectra (see Sherman and Waite (1985) for the description of these bands). Nevertheless it is modulated by the refractive index of the surrounding medium (air/water). In the blue region, absorption bands are such that the variation for the volumetric component predominates. This explains the increase in the total reflectance when the surrounding medium changes from air to water. Conversely, in the red region bands, the dominance swings from the specular component to the volumetric one: the total reflectance decreases, goes through a minimum, then increases.

These effects are stronger for the samples with higher contents of iron oxy-hydroxides. Since sample 4 has a very low content of oxy-hydroxides, its reflectance spectrum decreases almost homotheticaly when its moisture rate increases. These results are supported by the measurement of the reflectance spectra (dry and

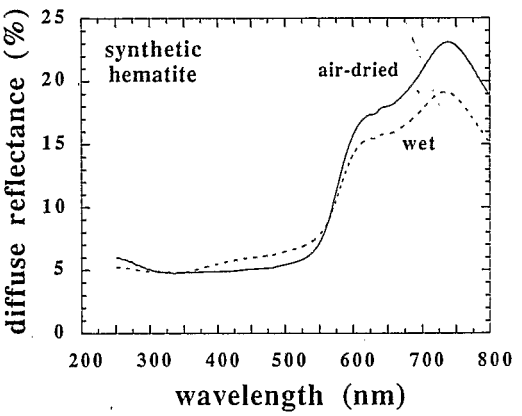

FIG. 6. Reflectance spectra of a synthetic hematite. (—) air-dried) and (- - -) wet. Note the crossing near 560 nm.

water saturated states) of both synthetic hematite and a natural kaolinite from USA-Georgia. The reflectance spectra of the synthetic hematite air-dried and water-saturated show a crossing at 560 nm (Fig. 6). On the contrary the spectra of the kaolinite are almost homothetic (spectra not shown). Now, let us consider the intermediate states. From "oven-dried" state to "water-saturated" state the pore space is progressively filled with water as described in *The shrinkage curve of a soil.* From the oven-dried state to pF 4.2, which generally corresponds to the air-entry point in the microporosity, only a part of the microporosity is full of water. In this case, part of the incident radiation meets a water surface. Since the reflectance of water is very low (4% at 90° incidence) the total radiation reflected by the soil decreases. The higher the initial reflectance (≫4%) the more important the decrease. Before the radiation is reflected back it meets a large number of interfaces which are of three types (air-soil material, air-water, water-soil material). Reflexion at these interfaces greatly decreases the diffuse reflectance (Prost et al. 1983). For lower pF values, the grains are covered by water films of increasing thickness. The number of different interfaces met by the radiation decreases. Variations in volumetric and specular reflectances, as discussed for water saturated samples, become important relatively to the variation due to reflexion at the interfaces. This leads to the crossing of the spectra and to the difference in their behavior from one wavelength to another and from a soil to another.

Results of Color Measurements

Chromaticity diagram

The points corresponding to the soil samples have been plotted on the chromaticity diagram (Fig. 1). The points for the same sample at different moisture contents lie on a straight line. The chromaticity coordinates (x and y) generally decrease when moisture content increases. However, the decrease is not monotonic, especially for high rates (pF 2.5 and 2.0). On the other hand, the four straight lines corresponding to the four soil samples do not intersect at the same point. The chromaticity coordinates of a sample, measured at a lapse of time of thirty minutes, increase implying a decrease of the moisture content. The slopes of the straight lines corresponding to samples 2, 3, and 4 cannot be distinguished at a confidence level of 95%. None of these straight lines passes by the point C, representing the C-illuminant; the main consequence is that the dominant wavelength (hue) changes with moisture content.

Purity and dominant wavelength variations with moisture contents

The dominant wavelength increases with moisture content, until pF 2.5 (see Fig. 7). This increase is more important for soil sample 1 which is more colored. The dominant wavelength increases from 594.2 nm for the oven-dried sample to 615 nm for the sample at pF 2.5. The increase of the dominant wavelength is not so important for the less colored samples 2 and 3. For the grey sample (4), the dominant wavelength variations are chaotic and are not shown.

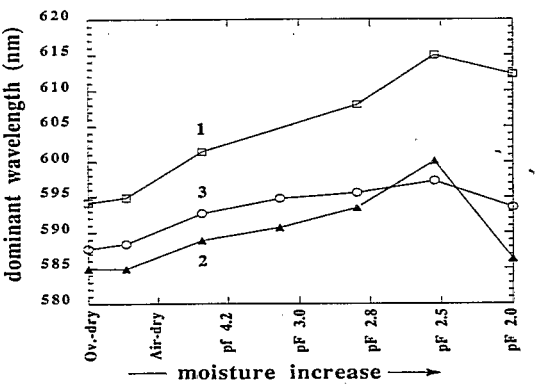

FIG. 7. Dominant wavelength λ_d for different moisture contents of samples 1(□), 2(△) and 3(○). Ov.-dry: oven-dried sample.

This chaotic behavior is due to the very low purity of sample (4). The dominant wavelength decreases after the pF 2.5.

The four soil samples studied undergo a systematic decrease of purity when the moisture content increases (see Fig. 8). This decrease is smaller for sample 4.

These results show that color variation due to moisture is not the same for "colored" and "uncolored" soils. They are more important for colored soils. Shields et al. (1968), using Munsell notations (Hue-Value-Chroma), showed that moisture does not induce changes in chroma (purity) and hue (dominant wavelength); they reported that their results differed from those cited in the references 18 and 19 in Shields et al. (1968). They attributed this disagreement to the differences in the preparation of the samples; it is probably due to the difference in nature and in chromaticity of the samples studied. As has been shown, iron oxides influence the extent and nature of the moisture-induced changes in color.

The variations of purity due to moisture are much greater than those which are due to the lamella. The relative variation of purity due to the lamella is about −9.4% for the Fe-sandstone sample, and it is only −5.2% for microgranite. This variation should be compared with that of the purity of moist samples relative to those oven-dried. At pF 2.5 the purity changed respectively by −57.8%, −72.2%, −56.6% and −84.3%, respectively, for soils (1, 2, 3, and 4).

The luminance decreases irregularly and not linearly with moisture content. The variations due to the lamella (−14% and −16%, respectively, for Fe-sandstone and microgranite) and those induced by moisture content are not very different (−21%, −25.4%, −27.7% and −14.3% at pF 2.5, respectively, for soils 1, 2, 3, and 4). Since the luminance is affected by the lamella, the results are not represented.

It should be pointed out that these color variations must be taken into account, when calculating color indices such as the redness rate (Barron and Torrent 1986; Torrent et al. 1983) for estimating the oxy-hydroxide content (ex. hematite) in laboratory studies as well as in remote sensing applications.

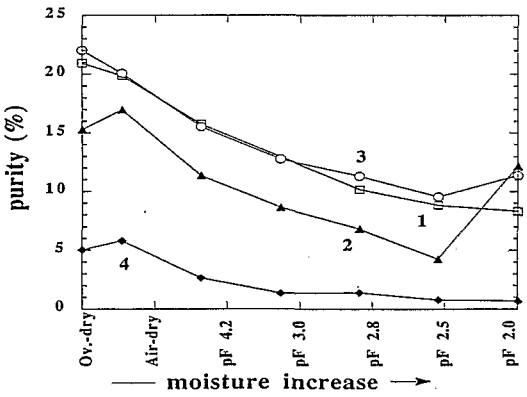

FIG. 8. Color purity for different moisture contents of samples 1(□), 2(△), 3(○) and 4(♦). Ov.-dry: oven-dried sample.

CONCLUSIONS

This study shows that the modification of the spectral properties of a soil when moistened depends upon its mineral components. However, many studies in the literature show that the reflectance of soils, in the visible range, undergoes quasi-homothetic variations against moisture content, which means, concerning their color, a decrease of the luminance when the moisture content increases but no significant changes in the dominant wavelength or in the purity (Bowers and Hanks 1965, Shields et al. 1968). These results hold for soils having featureless reflectance spectra, i.e., without absorption bands. This study shows that the spectral behavior versus moisture is more complex for lateritic soils since they contain oxy-hydroxides producing absorption bands between 400 nm and 700 nm. Any material containing absorbent species in the visible spectral region should induce similar reflectance variations when it is moistened.

There is a shift of the hue towards the red at high rates of moisture, and a systematic decrease of the purity. The color variation is due to a variation of reflectance which depends on the water content and its distribution into the macro and micro soil systems of porosity; this distribution is fixed by the texture and the structure of the soil. The reflectance of the lateritic soils studied, near 420 nm and near 540 nm, passes through two minima for the moisture content corresponding to the pF 4.2 which in turn, corresponds to the air-entry point into the micropores. Now, the air-entry point is very important for the hydric potential of soils in the sense that, for a higher dehydration, water still present in

the soil can no longer be absorbed, i.e., used by the vegetation.

In order to interpret these nonlinear spectral variations, one must take into account the fact that water is a medium with refractive index higher ($N = 1.33$) than that of air ($N = 1$). As water is transparent in the visible range, it only changes the refractive index of the immersion medium, that is air for dry soils and water for water saturated soils. This change in the refractive index of the immersion medium induces changes in the reflectance spectra depending on the existence, the location, and the intensity of absorption bands. As a matter of fact, the absorbency of the different mineral components of soils determines the contribution of each of the two main reflectance components to the total reflectance: the volumetric reflectance increases with the refractive index of the immersion medium and decreases when the minerals are highly absorptive, whereas the specular component behaves in the opposite way. The predominance of one of these two reflectance components governs the behavior of the total reflectance.

Therefore, there is a close relation between the spectral properties and the pedo-hydric behavior of soils which must be quantified precisely by shrinkage-curve recording and, simultaneously, spectral reflectance measurements, for different moisture rates. Then, this relation, may be used to measure pedo-hydric parameters, such as the hydric potential, and to derive applications of remote sensing for agriculture and soil science.

REFERENCES

Barron, V., and J. Torrent. 1986. Use of the Kubelka-Munk theory to study the influence of iron oxides on soil color. J. Soil Sci. 37:499–510.

Bertuzzi, P., G. Rauws, and D. Courault. 1990. Testing roughness indices to estimate soil surface roughness changes due to rainfall. Soil & Tillage Res. 17:87–99.

Bocquier, G., J. P. Muller, and B. Boulangé. 1984. Les laterites. Connaissances et perspectives actuelles sur les mécanismes de leur différenciation. Livre Jubilaire du Cinquantenaire. Association Française pour l'Etude du Sol. pp. 123–134.

Bohren, C. F. 1987. Clouds in a glass of beer. John Wiley & Sons, New York.

Boiffin, J. 1984. La dégradation structurale des couches superficielles du sol sous l'action des pluies. Thèse de docteur-ingénieur de l'INAPG. Paris. 320 p. + annexes.

Bowers, S. A., and R. J. Hanks. 1965. Reflection of radiant energy from soils. Soil Science. 100:130–138.

Bradeau, E. 1988. Méthode de caractérisation pédohydrique des sols basée sur l'analyse de la courbe de retrait. Cah. Orstom. Sér. Pédol., XXIV, 179–180.

Camargo, M. N., E. Klant, and J. H. Kauffman. 1987. Sistema braseileiro de classifiçào de solos. Boletim Informativo da Soc. Bras. Ci. Solo. 12 (1):11–33.

Cambier, P., and R. Prost. 1981. Etude des associations argile-oxyde: organisation des constituants d'un matériau ferralitique. Agronomie, 1 (9):713–722.

Cervelle, B., J. M. Malézieux, and R. Caye. 1977. Expression quantitative de la couleur, liée au spectre de réflectance diffuse, de quelques roches et minéraux. Bull. Soc. Fr. Minéral. Cristallogr. 100:258–262.

Cierniewski, J. 1983. Influences des structures de sol motteuse sur la réponse spectrale des sols. 2eme Coll. Int. "Signatures Spectrales d'Objets en Télédétection. INRA, Bordeaux, pp. 141–148.

Cierniewski, J. 1985. Relation between soil moisture tension and spectral reflectance of different soil in visible and near-infrared range. Proc. 3rd Int. Coll. on Spectral Signatures of Objects in Remote Sensing. Les Arcs, France, 16–20 Dec., (ESA SP-247).

Cierniewski, J. 1987. A model of soil surface roughness influence on the spectral response of bare soils in the visible and near-infrared range. Remote Sens Environ. 23:97–115.

EMBRAPA: Empresa Brasileira de Pesquisa Agropecuaria-SNLCS, Manual de methodos de analise de solos, Rio de Janiero, vol. I. 1979.

Epiphanio, J-C-N, and I. Vitorello. 1984. Inter relationships between view angles and surface moisture and roughness conditions in fields measured radiometer reflectance of an oxisol. 2eme Coll. Int. "Signatures Spectrales d'Objets en télédétection." Bordeaux, 12–16 Sept. 1983, Ed. INRA Publi.

Giraldez, J. V., G. Sposito, and C. Delgado. 1983. A general soil volume change equation: I. The two parameters model. Soil Sci. Soc. Am. J. 47:419–422.

Guidez, J. E., and R. Langohr. 1978. Some characteristics of pseudo-silts in a soil toposequence of Llanos Orientales (Venezuela). Pedologie, XXVII, 1, p. 118–131.

Harrisson, J. B. 1933. The katamorphism of igneous rock under humid tropical conditions. Imperial Bureau of Soil Science. Harpenden, England.

Hunt, G. R., and R. K. Vincent. 1968. The behavior of spectral features in the infrared emission from particulate surfaces of various grain sizes. J. Geophys. Res. 73 (n°18):6038–6046.

Macedo, J., R. B. Bryant. 1987. Morphology, mineralogy and genesis of a hydrosequence of oxisols in Brazil. Soil Sci. Soc. Am. J. 51:690–698.

Maquet, M., B. D. Cervelle, and G. Gouet. 1981. Signatures of Ni^{2+} and Fe^{3+} in the optical spectra of limonitic ore from New Caledonia: Application to the determination of the nickel content. Miner-

alium Deposita. 16:357–373.

McGarry, D., and I. G. Daniels. 1987. Shrinkage curve indices to quantify cultivation effects on soil structure of a vertisol. Soil Sci. Soc. Am. J. 51:1575–1580.

Mehra, O. P., and M. L. Jackson. 1960. Iron oxide removal from soils and clays by a dithionite-citrate system buffered with sodium bicarbonate. *In* Clays and Clay Minerals (Proc. 7th Nat. Conf.) Swineford A (ed.). Pergamon Press, New York, pp 317–327.

Mitchell, J-K., and B. Jones. 1978. Micro-relief surface depression storage changes during rainfall events and their application to rainfall-run off models. Water Res. Bull. 14:777–802.

Prost, R., C. King, and T. Lefebvre D'Hellencourt. 1983. Propriétés de réflexion de pâtes de kaolinites en fonction de leur teneur en eau. Clay Miner. 18:193–204.

Schwertmann, U. 1964. Differenzierung der Eisenoxide des Bodens durch photochemische Extraktion mit saurer Ammoniumoxalat-lösung. Z. Pflanzenernaehr, Dueng Bodenkd. 105:194–202.

Sherman, D. M., and T. D. Waite. 1985. Electronic spectra of Fe^{3+} oxides and oxides hydroxides in the near IR to near UV. Am. Mineral. 70:1262–1269.

Shields, J. A., E. A. Paul, R. J. St. Arnaud, and W. K. Head. 1968. Spectrophotometric measurement of soil color and its relationship to moisture and organic matter. Can. J. Soil Sci. 48:271–280.

Torrent, J., U. Schwertmann, H. Fechter, and F. Alferez. 1983. Quantitative relationships between soil color and hematite content. Soil Science. 136:354–358.

Vincent, R. K., and G. R. Hunt. 1968. Infrared reflection from mat surfaces. Appl Optics. 7:53–59.

Wendlandt W. WM., and H. G. Hecht. 1966. Reflectance spectroscopy. John Wiley & Sons, New York.

Wyszecki, G., and W. S. Stiles. 1982. Color science: Concepts and methods, quantitative data and formulae, 2nd Ed. John Wiley & Sons, New York.